

K. C. C. Pires  · S. Appannababu · R. Lichtenthäler

Determination of the ${}^6\text{He}$ Nuclear Radius from the Total Reaction Cross Section of ${}^6\text{He} + {}^9\text{Be}$

Received: 14 December 2015 / Accepted: 14 March 2016 / Published online: 5 April 2016
© Springer-Verlag Wien 2016

Abstract A new method to obtain the nuclear radius from low energies total reaction cross section measurements is presented. Elastic scattering angular distributions of ${}^6\text{He}$ on ${}^9\text{Be}$ at two energies, namely, $E_{\text{cm}} = 9.72$ and 12.78 MeV, were analysed previously and the total reaction cross sections obtained are used to assess the ${}^6\text{He}$ nuclear interaction radius. A comparison with the radius of the ${}^6\text{He}$ obtained at higher energies is presented.

1 Introduction

In a recent work [1], the ${}^6\text{He} + {}^9\text{Be}$ elastic angular distributions were analysed by Optical Model (OM), Coupled Channels (CC), 3-body and 4-body Continuum-Discretized Coupled-Channels (CDCC) calculations. The total reaction cross sections (for more details, see Ref. [2]) were obtained from each of the models and their average value and standard deviation were used to calculate the reduced reaction cross sections with a method that removes the geometric and Coulomb barrier effects, which allows a comparison between different systems at different energies [3,4]. The ${}^6\text{He}$ reduced reaction cross sections were compared with several other systems induced by light projectiles, all of them on ${}^9\text{Be}$ target. As a result, the exotic system apparently presents a higher reduced reaction cross section than stable systems [2].

In order to study the dependence of the observed enhancement with the target mass, we extended the analysis to the ${}^6\text{He}$ scattering on heavier targets from ${}^9\text{Be}$ [2] to ${}^{27}\text{Al}$ [5], ${}^{58}\text{Ni}$ [6], and ${}^{120}\text{Sn}$ [7]. The results showed a weak, but considerable, enhancement of $\Delta\sigma = 22(7)\%$ for 16.2 MeV and $31(18)\%$ for 21.3 MeV in the total reaction cross section for ${}^6\text{He} + {}^9\text{Be}$ system in comparison with $\Delta\sigma = 60\%$ observed for ${}^6\text{He}$ scattered on heavy targets [2]. The enhancement of the total reaction cross section with the target mass is expected, since reactions such as Coulomb breakup, inelastic excitations and neutron transfer reactions can take place in the long range Coulomb field.

In particular, an important point in this analysis is to investigate whether one can obtain the ${}^6\text{He}$ nuclear radius from these cross section measurements. It is well-known that, at high energies ($E \approx 790$ A MeV), the total reaction cross section is related to the radius of the system through a simple geometric relation: $\sigma_R = \pi R_I^2$ where R_I is the sum of the projectile and target radii [8] and is called interaction radius.

This terminology stems from the fact that the radius obtained directly from the total reaction cross section is not the nuclear radius itself, as defined by the matter distribution of the nuclei, but it includes all the interactions

K. C. C. Pires (✉) · S. Appannababu · R. Lichtenthäler
Instituto de Física, Universidade de São Paulo, C.P. 66318, São Paulo 05389-970, Brazil
E-mail: kelly@if.usp.br
Tel.: +55-11-30916939
Fax: +55-11-26480686

R. Lichtenthäler
E-mail: rubens@if.usp.br

between the target and the projectile as, for example, interactions in the long range Coulomb field, where there is no overlapping between the nuclear matter of projectile and target. As a consequence, the radius obtained from this simple geometric relation can be larger than the nuclear radius, defined as the radius where the nuclear density reaches one half of the its saturation value.

At high energies and for light targets the effect of reactions occurring in the Coulomb field are negligible and, therefore, the nuclear interaction radius should be, approximately equal to the nuclear radius [8]. However, as the energy decreases approaching the Coulomb barrier, the effect of those long range interactions may become very large. As a consequence, the interacting radius obtained directly from total reaction cross section measurements using the above geometrical formula will result in a radius much larger than the actual nuclear matter distribution radius.

Here, we present a new method to obtain the nuclear radius from low energy total reaction cross sections measurements. The method is applied to ${}^6\text{He}+{}^9\text{Be}$ and ${}^9\text{Be}+{}^9\text{Be}$ data. The ${}^6\text{He}$ nuclear radius is extracted and compared with results from high energies.

2 The ${}^6\text{He}$ Nuclear Radius

The ${}^6\text{He}+{}^9\text{Be}$ angular distributions were analysed previously with Optical Model (OM), Coupled Channels (CC), 3b- and 4b- Continuum-Discretized Coupled-Channels (CDCC) calculations [1]. The results are presented in Fig. 1.

One sees in Fig. 1 that there is a considerable discrepancy among the different calculations. In particular the 3-body CDCC calculations seem to reproduce better the data than the 4-body CDCC mainly at 21.3 MeV backward angles, showing that, probably, the theoretical errors are at least of the same order of the experimental ones. Optical Model presents the best fit to the data because there are free adjusted parameters.

The total reaction cross sections obtained from these analysis are shown in Table 1, and basically, agree with each other except for the OM value at 21.3 MeV which is considerably larger than the other calculations.

The problem of obtaining the nuclear radius from total reaction cross section measurements at low energies is a challenge. It has been recognized recently that a simple geometric formula (see Eq. 1 below) gives reasonable values of the total reaction cross sections, provided that one uses the Coulomb barrier radius R_B and Coulomb

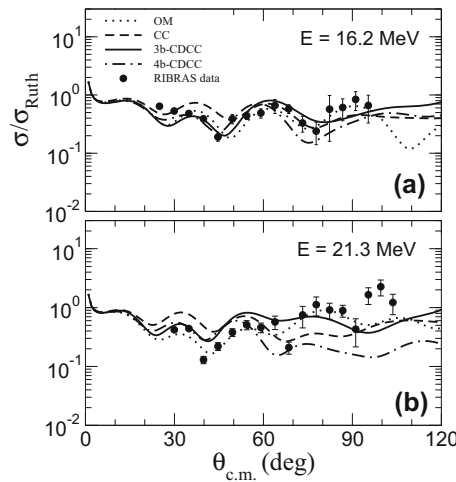


Fig. 1 Elastic scattering angular distribution for ${}^6\text{He}+{}^9\text{Be}$ at **a** $E_{\text{lab}} = 16.2$ MeV and **b** 21.3 MeV [1,2]. The solid circles are the RIBRAS data, the dotted line is the OM, the dashed line is the CC, the solid line is the 3b-CDCC and the dotted-dashed line is the 4b-CDCC calculation. Figure taken from Ref. [2]

Table 1 The ${}^6\text{He}+{}^9\text{Be}$ total reaction cross sections, σ_R in fm^2 , and the average values with errors

E_{lab} (MeV)	σ_R^{OM} (fm^2)	σ_R^{CC} (fm^2)	$\sigma_R^{3b-CDCC}$ (fm^2)	$\sigma_R^{4b-CDCC}$ (fm^2)	$\bar{\sigma}_R$ (fm^2)
16.2	151.3	144.5	148.8	164.3	152.2 (8.5)
21.3	194.4	144.9	148.3	164.8	163.1 (22.6)

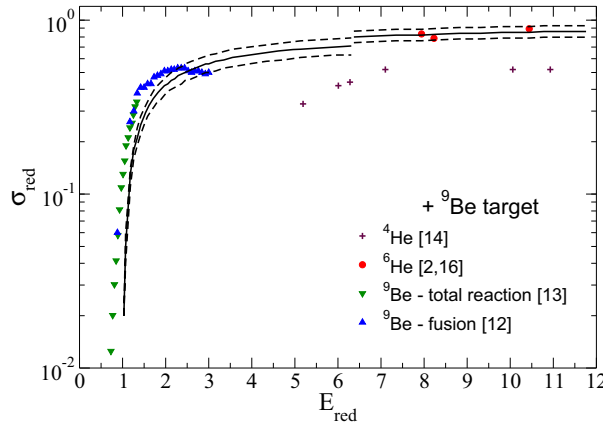


Fig. 2 Reduced total reaction cross section for different systems induced by exotic, weakly and strongly bound projectiles [2, 12–14, 16]. Solid and dotted lines are the predictions from Eq. 1 for ${}^6\text{He} + {}^9\text{Be}$ and ${}^9\text{Be} + {}^9\text{Be}$ system, respectively

barrier strength V_B parameters obtained from double folding potential calculations such as, for instance, the São Paulo potential [9].

The Coulomb barrier radius, R_B , can be obtained from σ_R by using the geometric formula for the total reaction cross section:

$$\sigma_R = \pi R_B^2 \left(1 - \frac{V_B}{E} \right) \quad (1)$$

More recently, a simple analytic formula was developed [10, 11] which provides the Coulomb barrier strength V_B and Coulomb barrier radius R_B parameters equivalent to the ones obtained from double folding potential calculations.

$$V_B = \frac{Z_p Z_t e^2}{R_B} - \frac{15}{x + 1} \quad (2)$$

$$\text{where } x = \frac{27.1 (A_p^{1/3} + A_t^{1/3})^2}{Z_p Z_t}$$

and

$$R_B = R + 0.65 \ln [x] \quad (3)$$

Equation 3 provides the relation between the Coulomb barrier radius R_B and the nuclear interaction radius R , that we are interested in.

We applied this method to the present ${}^6\text{He} + {}^9\text{Be}$ data. We used as starting point the average values for σ_R as presented in Table 1, and then R_B from Eq. 1. The Coulomb barrier for the ${}^6\text{He} + {}^9\text{Be}$ system, $V_B = 1.22$ MeV, was obtained using Eqs. 2 and 3 with $R = 1.3(A_p^{1/3} + A_t^{1/3})$. Finally, the ${}^6\text{He}$ nuclear radius, $R(p)$, is obtained from Eq. 3, since $R = R(p) + R(t)$ and $R(t)$ is the target radius.

The ${}^9\text{Be}$ target radius was calculated with the same method using ${}^9\text{Be} + {}^9\text{Be}$ data from Refs. [12, 13], that includes the total reaction and fusion cross section data. Figure 2 presents the reduced cross sections for ${}^6\text{He}$, ${}^4\text{He}$ and ${}^9\text{Be}$ projectiles on ${}^9\text{Be}$ target [2, 12–15].

The reduced energies and cross sections of Fig. 2 were obtained by dividing the center of mass energies by V_B and the cross sections by πR_B^2 with V_B and R_B from Eqs. 2 and 3 and $R = 1.3(A_p^{1/3} + A_t^{1/3})$. We remark (see Fig. 2) that the total reaction and fusion cross sections for the ${}^9\text{Be} + {}^9\text{Be}$ system are very much the same at the energies of the measurements.

In Fig. 2, the solid curves have been obtained using Eq. 1 with $R_B = 6.6$ fm and $R_B = 7.6$ fm, respectively, for ${}^9\text{Be} + {}^9\text{Be}$ and ${}^6\text{He} + {}^9\text{Be}$ system. The dashed curves are an estimation of the error bars in R_B . For V_B we used the Eq. 2 with $R = 1.3(A_p^{1/3} + A_t^{1/3})$. The value of the ${}^9\text{Be}$ radius obtained is 2.40 ± 0.18 fm, in agreement with 2.45 ± 0.01 fm from Ref. [8]. The uncertainties in R_B were estimated by the two dashed curves presented in Fig. 2. The uncertainty in $R({}^6\text{He})$ are affected by both, the uncertainties in R_B and from the ${}^9\text{Be}$ radius determination.

The value for ${}^6\text{He}$ nuclear radius was obtained for the three energies (see Table 2) and the average result is 2.45 ± 0.20 fm. In Ref. [8], a radius of 2.21 ± 0.06 fm was obtained for ${}^6\text{He}$ nucleus at 790 MeV/nucleon. In Ref. [17] a value of 2.56 fm is obtained for the ${}^6\text{He}$ rms (root mean square) radius.

Table 2 The Coulomb barrier radius (R_B), x , nuclear interaction radius (R) and ${}^6\text{He}$ radius ($R(p)$) values

System	E_{lab} (MeV)	E_{cm} (MeV)	R_B (fm)	V_B^{cm} (MeV)	x	R (fm)	$R(p)$ (fm)
${}^6\text{He}+{}^9\text{Be}$	16.2	9.72	7.44 (0.21)	1.22	51.45	4.88 (0.21)	2.49 (0.28)
	16.8	10.08	7.21	1.22	51.45	4.65	2.26
	21.3	12.78	7.56 (0.52)	1.22	51.45	5.02 (0.52)	2.62 (0.55)
${}^9\text{Be}+{}^9\text{Be}$	—	—	6.60 (0.37)	2.54	29.31	4.40 (0.37)	2.40 (0.18)

3 Conclusions

A simple formalism is presented which allows the determination of the nuclear matter distribution radius directly from low energy total reaction measurements. The formalism is applied to fusion and total reaction cross sections measurements for the systems ${}^9\text{Be}+{}^9\text{Be}$ and ${}^6\text{He}+{}^9\text{Be}$ systems allowing the determination of the ${}^9\text{Be}$ and ${}^6\text{He}$ radii. The results agree well with previous measurements at high energies.

Acknowledgments The authors acknowledge the Fundação de Amparo à Pesquisa do Estado de São Paulo (FAPESP) and Conselho Nacional de Desenvolvimento Científico e Tecnológico (CNPq) for financial support.

References

1. Pires, K.C.C., et al.: Experimental study of ${}^6\text{He}+{}^9\text{Be}$ elastic scattering at low energies. *Phys. Rev. C* **83**, 064603-1–064603-8 (2011)
2. Pires, K.C.C., et al.: Total reaction cross section for the ${}^6\text{He}+{}^9\text{Be}$ system. *Phys. Rev. C* **90**, 027605-1–027605-4 (2014)
3. Gomes, P.R.S., et al.: Fusion, reaction and break-up cross sections of weakly bound projectiles on ${}^{64}\text{Zn}$. *Phys. Lett. B* **601**, 20 (2004)
4. Gomes, P.R.S., Lubian, J., Padron, I., Anjos, R.M.: Uncertainties in the comparison of fusion and reaction cross sections of different systems involving weakly bound nuclei. *Phys. Rev. C* **71**, 017601 (2005)
5. Benjamin, E., et al.: Elastic scattering and total reaction cross section for the ${}^6\text{He}+{}^{27}\text{Al}$ system. *Phys. Lett. B* **647**, 30 (2007)
6. Morcelle, V., et al.: Four-body effects in the ${}^6\text{He}+{}^{58}\text{Ni}$ scattering. *Phys. Lett. B* **732**, 228–232 (2014)
7. de Faria, P.N., et al.: Elastic scattering and total reaction cross section of ${}^6\text{He}+{}^{120}\text{Sn}$. *Phys. Rev. C* **81**, 044605 (2010)
8. Tanihata, I., et al.: Measurements of interaction cross sections and radii of He isotopes. *Phys. Lett. B* **160**(6), 380 (1985)
9. Yang, X.P., Zhang, G.L., Zhang, H.Q.: Systematic study of reaction functions of weakly bound nuclei. *Phys. Rev. C* **87**, 014603 (2013)
10. Freitas, A.S., et al.: Woods–Saxon equivalent to a double folding potential. [arXiv:1508.00557v2](https://arxiv.org/abs/1508.00557v2) (2015)
11. Freitas, A.S., et al.: Woods–Saxon equivalent to a double folding potential. *Braz. J. Phys.* (2015). doi:[10.1007/s13538-015-0387-y](https://doi.org/10.1007/s13538-015-0387-y)
12. Mukherjee, A., Dasmahapatra, B.: Fusion cross sections for ${}^7\text{Li}+{}^{11}\text{B}$ and ${}^9\text{Be}+{}^9\text{Be}$ reactions at low energies. *Nucl. Phys. A* **614**, 238 (1997)
13. Lahlou, F., Cujec, B., Dasmahapatra, B.: Cross section measurements at subbarrier for the ${}^9\text{Be}+{}^9\text{Be}$ system at subbarrier energies. *Nucl. Phys. A* **486**, 189 (1988)
14. Taylor, R.B., Fletcher, N.R., Davis, R.H.: Elastic scattering of 4–20 MeV alpha particles by ${}^9\text{Be}$. *Nucl. Phys.* **65**, 318 (1965)
15. Brady, F.P., Jungerman, J.A., Young, J.C.: Elastic alpha-particle scattering at 8.75, 9.35 and 10.15 MeV. *Nucl. Phys. A* **98**, 241 (1967)
16. Majer, M., Raabe, R., Milin, M., et al.: ${}^6\text{He}+{}^9\text{Be}$ reactions at 16.8 MeV. *Eur. Phys. J. A* **43**, 153 (2010)
17. Karataglidis, S., Dortmans, P.J., Amos, K., Bennhold, C.: Alternative evaluations of halo in nuclei. *Phys. Rev. C* **61**, 024319 (2000)